

Exponentially Enhanced Scheme for the Heralded Qudit GHZ State in Linear Optics

Seungbeom Chin*

Department of Electrical and Computer Engineering,
Sungkyunkwan University, Suwon 16419, Korea

Junghee Ryu

Center for Quantum Information R&D, Korea Institute of
Science and Technology Information, Daejeon 34141, Korea
Division of Quantum Information, KISTI School,
Korea University of Science and Technology, Daejeon, 34113, Korea

Yong-Su Kim

Center for Quantum Information, Korea Institute of Science and Technology (KIST), Seoul, 02792, Korea
Division of Quantum Information Technology, KIST School,
Korea University of Science and Technology, Seoul 02792, Korea

High-dimensional multipartite entanglement plays a crucial role in quantum information science. However, existing schemes for generating such entanglement become increasingly complex and costly as the dimension of quantum units increases. In this work, we overcome the limitation by proposing a significantly enhanced linear optical heralded scheme that generates the d -level N -partite GHZ state with single-photon sources and their linear operations. Our scheme requires dN photons to generate the target state with substantially improved success probability from previous schemes. It employs linear optical logic gates compatible with any qudit encoding system and can generate generalized GHZ states with installments of beamsplitters. With efficient generations of high-dimensional resource states, our work opens avenues for further exploration in high-dimensional quantum information processing.

Introduction.— A qubit, which is comprised of a two-level quantum system and functions, is the quantum counterpart to the classical bit. It is generally considered the basic unit that stores and delivers information in quantum tasks. However, many natural systems have higher degrees of freedom, such as frequencies and paths of particles. Quantum information theory provides a new way of encoding such multi-level systems, which is called the *qudit*. Qudits provide larger Hilbert spaces than qubits for encoding and manipulating information. Higher-dimensional quantum systems exhibit distinctive properties that are unattainable with qubit-based systems such as contextuality [1]. They also provide a handy platform to simulate several quantum systems [2, 3].

Numerous advantages arise from entangling multiple quantum units in quantum information processing. The Bell state of qubits facilitates quantum enhancements over classical counterparts [4, 5]. Beyond two-qubit systems, quantum entanglement in multipartite and/or higher-dimensional systems is essential for new quantum technologies such as quantum cryptography, reduction of communication complexity, quantum communication protocols, and random number generation [6–10].

On the other hand, the intricate structure of qudit multipartite entanglement brings about several theoretical and practical challenges such as classification problems according the separability of states [11] and the maximal quantum violation by non-maximally entangled qutrit bipartite states [12, 13]. Another crucial problem lies on the *generation of qudit multipartite entangled states* for the practical performances of quantum tasks. The increased degrees of freedom in the system generally make the generation process significantly more complex and expensive.

We contribute to overcoming this limit by providing a *magnificently enhanced heralded scheme for generating the qudit multipartite entanglement in linear optical networks (LONs)*. The LON is one of promising systems that can feasibly generate quantum resource states. Non-destructive entanglement generations by heralding are possible in LONs by utilizing ancillary particles to herald the successful operation events without direct detections of the target states. Therefore, photons entangled by heralding become proper resources for quantum computations with multiple gates [14, 15] and also facilitates loophole-free Bell tests [16, 17]. However, the number of additional particles and modes that the

heralded schemes require increases as the dimension of entanglement becomes higher, which makes the circuit structures much more intricate. Therefore, it is prerequisite to design optimized circuits that achieve the target state with minimal resources for the efficient high-dimensional quantum information processing.

In this work, we propose a heralded scheme to generate one of essential qudit multipartite entangled states, i.e., the N -partite d -level GHZ state $|GHZ_N^d\rangle$:

$$|GHZ_N^d\rangle = \frac{1}{\sqrt{d}} \sum_{j=0}^{d-1} |j\rangle_1 \otimes \cdots \otimes |j\rangle_N \quad (1)$$

where $|j\rangle_k$ denotes the k th qudit being in the j th state. The qudit GHZ state reveals intriguing non-classical properties of N -partite d -level systems such as the GHZ paradox [18–21] and Bell inequalities [22]. It also becomes a resource state to generate qudit cluster states for the high-dimensional measurement-based quantum computing (MBQC) [23–25].

Heralded schemes for the qudit GHZ state in various physical setups have been proposed, e.g., with single-photon sources and linear optical operators [25], EPR sources [26], or an array of non-interacting photon emitters [27]. Among them, Ref. [25] suggested a linear optical heralded scheme based on the zero-transmission laws (ZTL) in quantum Fourier transforms (QFTs). However, it suffers from low efficiency and exponentially increasing photon numbers as N and d grows.

In this work, we propose a scheme that generates the GHZ state of any N and d with the most feasible optical elements, i.e., single photons and linear optical operators as in Ref. [25]. Our scheme has several manifest advantages over formerly suggested schemes: First, it is an efficient circuit with significantly less photons (dN photons for $|GHZ_N^d\rangle$) and exponentially higher success probability than that in Ref. [25]. Second, it can easily control the probability amplitudes of each term in the GHZ state by simply placing beamsplitters on the paths of photons, which result in the generation of the generalized qudit GHZ state. Third, it consists of linear optical logic gates that any type of qubit encoding (e.g., optical angular momentum (OAM), multi-rail, time-bin, etc.) can establish.

Linear optical logic gates for generating $|GHZ_N^d\rangle$.— We first introduce a set of linear optical logic gates, which will compose our scheme. The list of the gates with their pictorial notations is

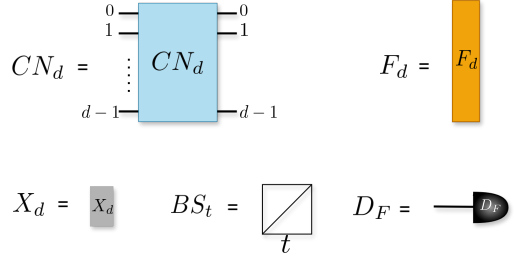


FIG. 1: The list of linear optical logic gates that will be used to design the qudit GHZ generating circuits.

given in Fig. 1.

1. CN_d : The d -level generalized CNOT gate between the spatial mode j ($\in \{0, 1, \dots, d\}$) and the internal state \tilde{s} ($\in \{\tilde{0}, \tilde{1}, \dots, \tilde{d}\}$), which works on states as

$$\begin{aligned} |\tilde{s}\rangle_j &= \hat{a}_{j,\tilde{s}}^\dagger |vac\rangle \\ \rightarrow CN_d |\tilde{s}\rangle_j &= |\tilde{s}\rangle_{j \oplus_d \tilde{s}} = \hat{a}_{j \oplus_d \tilde{s}, \tilde{s}}^\dagger |vac\rangle \end{aligned} \quad (2)$$

($\hat{a}_{j,\tilde{s}}^\dagger$ is a photon creation operator, $|vac\rangle$ is the vacuum state, and \oplus_d is the addition modular d). Its inverse \overline{CN}_d works as

$$\begin{aligned} |\tilde{s}\rangle_j &= \hat{a}_{j,\tilde{s}}^\dagger |vac\rangle \\ \rightarrow \overline{CN}_d |\tilde{s}\rangle_j &= |\tilde{s}\rangle_{j \ominus_d \tilde{s}} = \hat{a}_{j \ominus_d \tilde{s}, \tilde{s}}^\dagger |vac\rangle \end{aligned} \quad (3)$$

where \ominus_d is the subtraction modular d . These operators split states in the same spatial mode with different internal states into different spatial modes (see Appendix A for a more detailed explanation).

For $d = 2$, we can build these operators with polarized photons. By setting $\{H, V\} = \{0, 1\}$ (H =horizontal, V =vertical), CN_2 and \overline{CN}_2 are both implemented with a polarizing beam splitter (PBS).

2. F_d : The internal state Fourier-transformation gate,

$$F_d |\tilde{s}\rangle_j = |s\rangle_j = \frac{1}{\sqrt{d}} \sum_{r=0}^{d-1} e^{i\omega r} |\tilde{r}\rangle \quad (\omega = e^{i\frac{2\pi k}{d}}). \quad (4)$$

F_d changes the computational basis of the internal state into its Fourier-transformed basis. For $d = 2$, F_2 can be installed in the polarization encoding with a half-wave plate (HWP).

3. X_d : The d -level unitary generalization of σ_x in qubit,

$$X_d = \sum_{k=0}^{d-1} |k \oplus 1\rangle \langle k|, \quad (5)$$

under which $|k\rangle$ transforms to $|k \oplus 1\rangle$.

4. BS_t : A beamsplitter that transmits a photon with transitivity t .

5. D_F : Number resolving detections in the Fourier-transformed basis, i.e., measurements in $\{|s\rangle\}_{s=0}^{d-1}$ and postselections of the cases when only one particle arrives at the detector. This is achieved by combining F_d and CN_d , i.e.,

$$\text{---} \otimes D_F = \text{---} \otimes F_d \otimes CN_d \otimes \dots$$

where $\text{---} \otimes D_F$ denotes the particle-number-resolving detector.

Linear optical circuits for generating $|GHZ_N^d\rangle$.—

By combining the gates listed in Fig. 1, we can design a circuit that generates $|GHZ_N^d\rangle$ for any N and d . Our scheme is given in Fig. 2, which can be considered a linear optical installation of the boson subtraction scheme in Ref. [28] to generate the same target state. While Ref. [28] lacks how to furnish the qudit boson subtraction operators with real physical systems, we demonstrate that the elements of the boson subtraction scheme for $|GHZ_N^d\rangle$ can be translated to the linear optical logic gates to construct a physical qudit GHZ scheme with heralding. A more detailed explanation on the relation between the subtraction operator and our optical heralded scheme is given in Appendix B.

In each input mode of the circuit in Fig. 2, we inject d photons with different internal states in the same mode. The operation of each dashed box in the circuit corresponds to the boson subtraction of $(d-1)$ particles, hence $(d-1)N$ subtraction of photons in total. BS_t s are attached to control the probability amplitude of the target state, hence we can obtain different states in the class of generalized GHZ states by changing the transitivity of the BS_t s. It is worth noting that *our circuit inherits the cyclic symmetry of the qudit GHZ state*.

The success probability $P_{suc}(N, d)$ for generating $|GHZ_N^d\rangle$ is given by

$$P_{suc}(N, d) = d \left(\frac{d!}{d^d} \right)^{2N}. \quad (6)$$

When $d = 2$, by considering CN_2 and \overline{CN}_2 with PBS and F_d with HWP, this circuit corresponds to the qubit GHZ generation scheme proposed in Ref. [29]. Appendix B demonstrates how the circuit in Fig. 2 generates $|GHZ_N^d\rangle$ by heralding.

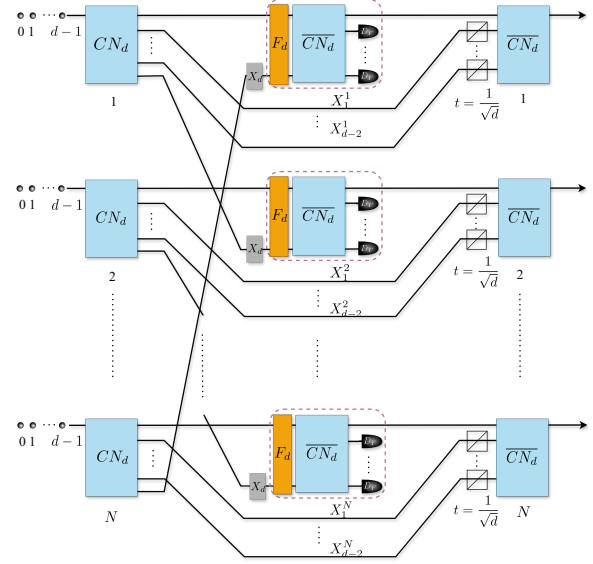


FIG. 2: The linear optical circuit that generates $|GHZ_N^d\rangle$. ABSs are attached at the end of the d sub-modes of the first spatial subsystem 1 to control the probability amplitudes of the terms in the target state, hence we can obtain the generalized qudit GHZ states.

$|GHZ_3^3\rangle$ example.— As proof of concept, we provide here a step-by-step analysis on the $N = d = 3$ example (Fig. 3). There are three spatial subsystems $\{a, b, c\}$ that has three sub-modes respectively, hence the photon creation operator is denoted as $\{\hat{a}_{j,s}^\dagger, \hat{b}_{k,r}^\dagger, \hat{c}_{l,t}^\dagger\}$ where $\{j, k, l\}$ denotes the spatial sub-modes and $\{s, r, t\}$ the qudit states $(j, k, l, s, r, t \in \{0, 1, 2\})$.

Step 1. Initial state preparation: We inject three photons of orthogonal internal states with each other into the 0th modes of a , b , and c respectively, hence the initial state is prepared as

$$\hat{a}_{0,0}^\dagger \hat{a}_{0,1}^\dagger \hat{a}_{0,2}^\dagger \hat{b}_{0,0}^\dagger \hat{b}_{0,1}^\dagger \hat{b}_{0,2}^\dagger \hat{c}_{0,0}^\dagger \hat{c}_{0,1}^\dagger \hat{c}_{0,2}^\dagger |vac\rangle. \quad (7)$$

Step 2. CN_3 operation: This operator works on the basis of $\{|\tilde{j}\rangle\}_{j=0}^2$, hence the initial state is trans-

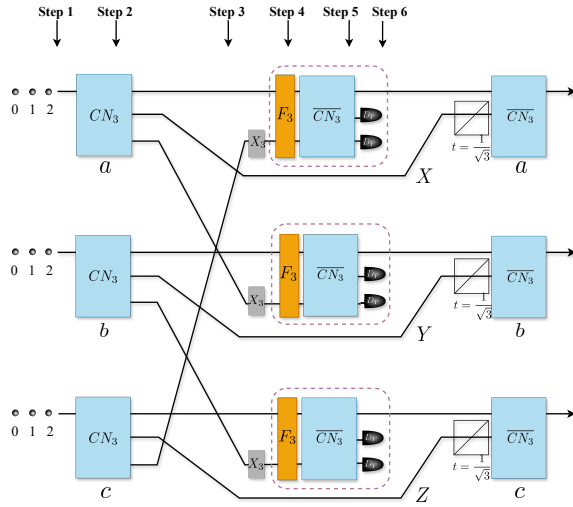


FIG. 3: $|GHZ_3^3\rangle$ example of our scheme. We need a BS with transitivity $\frac{1}{\sqrt{3}}$ on X , Y and Z to carve the extra amplitude of $|111\rangle$.

formed as

$$\begin{aligned} & \frac{1}{\sqrt{3}^9} (\hat{a}_{0,0}^{\dagger 3} + \hat{a}_{1,1}^{\dagger 3} + \hat{a}_{2,2}^{\dagger 3} - 3\hat{a}_{0,0}^{\dagger} \hat{a}_{1,1}^{\dagger} \hat{a}_{2,2}^{\dagger}) \\ & \times (\hat{b}_{0,0}^{\dagger 3} + \hat{b}_{1,1}^{\dagger 3} + \hat{b}_{2,2}^{\dagger 3} - 3\hat{b}_{0,0}^{\dagger} \hat{b}_{1,1}^{\dagger} \hat{b}_{2,2}^{\dagger}) \\ & \times (\hat{c}_{0,0}^{\dagger 3} + \hat{c}_{1,1}^{\dagger 3} + \hat{c}_{2,2}^{\dagger 3} - 3\hat{c}_{0,0}^{\dagger} \hat{c}_{1,1}^{\dagger} \hat{c}_{2,2}^{\dagger}) |vac\rangle \quad (8) \end{aligned}$$

Step 3. Rewiring: Now we rewire so that creation operators $\{\hat{a}_{1,1}^{\dagger}, \hat{b}_{1,1}^{\dagger}, \hat{c}_{1,1}^{\dagger}\}$ are sent to $\{\hat{X}_{\bar{1}}^{\dagger}, \hat{Y}_{\bar{1}}^{\dagger}, \hat{Z}_{\bar{1}}^{\dagger}\}$ and $\{\hat{a}_{2,2}^{\dagger}, \hat{b}_{2,2}^{\dagger}, \hat{c}_{2,2}^{\dagger}\}$ to $\{\hat{b}_{2,2}^{\dagger}, \hat{c}_{2,2}^{\dagger}, \hat{a}_{2,2}^{\dagger}\}$:

$$\begin{aligned} & \frac{1}{\sqrt{3}^9} (\hat{a}_{0,0}^{\dagger 3} + \hat{X}_{\bar{1}}^{\dagger 3} + \hat{b}_{2,2}^{\dagger 3} - 3\hat{a}_{0,0}^{\dagger} \hat{X}_{\bar{1}}^{\dagger} \hat{b}_{2,2}^{\dagger}) \\ & \times (\hat{b}_{0,0}^{\dagger 3} + \hat{Y}_{\bar{1}}^{\dagger 3} + \hat{c}_{2,2}^{\dagger 3} - 3\hat{b}_{0,0}^{\dagger} \hat{Y}_{\bar{1}}^{\dagger} \hat{c}_{2,2}^{\dagger}) \\ & \times (\hat{c}_{0,0}^{\dagger 3} + \hat{Z}_{\bar{1}}^{\dagger 3} + \hat{a}_{2,2}^{\dagger 3} - 3\hat{c}_{0,0}^{\dagger} \hat{Z}_{\bar{1}}^{\dagger} \hat{a}_{2,2}^{\dagger}) |vac\rangle \quad (9) \end{aligned}$$

Step 4. X_d and F_3 : Now the internal states of the creation operators go back to the basis of $\{|j\rangle\}_{j=0}^2$:

$$\begin{aligned} & \frac{1}{\sqrt{3}^9} (\hat{a}_{0,0}^{\dagger 3} + \hat{X}_{\bar{1}}^{\dagger 3} + \hat{b}_{2,0}^{\dagger 3} - 3\hat{a}_{0,0}^{\dagger} \hat{X}_{\bar{1}}^{\dagger} \hat{b}_{2,0}^{\dagger}) \\ & \times (\hat{b}_{0,0}^{\dagger 3} + \hat{Y}_{\bar{1}}^{\dagger 3} + \hat{c}_{2,0}^{\dagger 3} - 3\hat{b}_{0,0}^{\dagger} \hat{Y}_{\bar{1}}^{\dagger} \hat{c}_{2,0}^{\dagger}) \\ & \times (\hat{c}_{0,0}^{\dagger 3} + \hat{Z}_{\bar{1}}^{\dagger 3} + \hat{a}_{2,0}^{\dagger 3} - 3\hat{c}_{0,0}^{\dagger} \hat{Z}_{\bar{1}}^{\dagger} \hat{a}_{2,0}^{\dagger}) |vac\rangle \quad (10) \end{aligned}$$

Step 5. $\overline{CN_3}$

$$\begin{aligned} & \frac{1}{3^9} \left[(\hat{a}_{0,0}^{\dagger} + \hat{a}_{2,1}^{\dagger} + \hat{a}_{1,2}^{\dagger})^3 + \hat{X}_{\bar{1}}^{\dagger 3} + (\hat{b}_{2,0}^{\dagger} + \hat{b}_{1,1}^{\dagger} + \hat{b}_{0,2}^{\dagger})^3 \right. \\ & \left. - 3\sqrt{3}\alpha(\hat{a}_{0,0}^{\dagger} + \hat{a}_{2,1}^{\dagger} + \hat{a}_{1,2}^{\dagger})\hat{X}_{\bar{1}}^{\dagger}(\hat{b}_{2,0}^{\dagger} + \hat{b}_{1,1}^{\dagger} + \hat{b}_{0,2}^{\dagger}) \right] \\ & \times \left[(\hat{b}_{0,0}^{\dagger} + \hat{b}_{2,1}^{\dagger} + \hat{b}_{1,2}^{\dagger})^3 + \hat{Y}_{\bar{1}}^{\dagger 3} + (\hat{c}_{2,0}^{\dagger} + \hat{c}_{1,1}^{\dagger} + \hat{c}_{0,2}^{\dagger})^3 \right. \\ & \left. - 3\sqrt{3}\alpha(\hat{b}_{0,0}^{\dagger} + \hat{b}_{2,1}^{\dagger} + \hat{b}_{1,2}^{\dagger})\hat{Y}_{\bar{1}}^{\dagger}(\hat{c}_{2,0}^{\dagger} + \hat{c}_{1,1}^{\dagger} + \hat{c}_{0,2}^{\dagger}) \right] \\ & \times \left[(\hat{c}_{0,0}^{\dagger} + \hat{c}_{2,1}^{\dagger} + \hat{c}_{1,2}^{\dagger})^3 + \hat{Z}_{\bar{1}}^{\dagger 3} + (\hat{a}_{2,0}^{\dagger} + \hat{a}_{1,1}^{\dagger} + \hat{a}_{0,2}^{\dagger})^3 \right. \\ & \left. - 3\sqrt{3}\alpha(\hat{c}_{0,0}^{\dagger} + \hat{c}_{2,1}^{\dagger} + \hat{c}_{1,2}^{\dagger})\hat{Z}_{\bar{1}}^{\dagger}(\hat{a}_{2,0}^{\dagger} + \hat{a}_{1,1}^{\dagger} + \hat{a}_{0,2}^{\dagger}) \right] |vac\rangle \quad (11) \end{aligned}$$

Step 6. Postselections and feed-forward: After the postselection of the cases when each detector observes only one photon, the terms that contribute to the final states are

$$\begin{aligned} & \frac{1}{3^9} \left[6^3 \hat{a}_{0,0}^{\dagger} \hat{a}_{2,1}^{\dagger} \hat{a}_{1,2}^{\dagger} \hat{b}_{0,0}^{\dagger} \hat{b}_{2,1}^{\dagger} \hat{b}_{1,2}^{\dagger} \hat{c}_{0,0}^{\dagger} \hat{c}_{2,1}^{\dagger} \hat{c}_{1,2}^{\dagger} \right. \\ & + 6^3 \hat{a}_{2,0}^{\dagger} \hat{a}_{1,1}^{\dagger} \hat{a}_{0,2}^{\dagger} \hat{b}_{2,0}^{\dagger} \hat{b}_{1,1}^{\dagger} \hat{b}_{0,2}^{\dagger} \hat{c}_{2,0}^{\dagger} \hat{c}_{1,1}^{\dagger} \hat{c}_{0,2}^{\dagger} \\ & \left. - (3\sqrt{3})^3 \alpha^3 \hat{X}_{\bar{1}} \hat{Y}_{\bar{1}} \hat{Z}_{\bar{1}} (\hat{a}_{1,1}^{\dagger} \hat{a}_{2,1}^{\dagger} + \hat{a}_{1,2}^{\dagger} \hat{a}_{2,0}^{\dagger}) \right. \\ & \left. \times (\hat{b}_{1,1}^{\dagger} \hat{b}_{2,1}^{\dagger} + \hat{b}_{1,2}^{\dagger} \hat{b}_{2,0}^{\dagger})(\hat{c}_{1,1}^{\dagger} \hat{c}_{2,1}^{\dagger} + \hat{c}_{1,2}^{\dagger} \hat{c}_{2,0}^{\dagger}) \right] |vac\rangle \quad (12) \end{aligned}$$

After the postselection with D_{FS} and feedforwards, the final state becomes

$$\frac{6^3}{3^9} \left[|0,0,0\rangle - 3\sqrt{3}\alpha^3 |1,1,1\rangle + |2,2,2\rangle \right]. \quad (13)$$

Setting $\alpha = \frac{1}{\sqrt{3}}$, the final state becomes the tripartite qutrit GHZ state. The success probability is given by

$$P_{suc}(3,3) = \left(\frac{2}{9}\right)^6 \sim 3.6 \times 10^{-4}. \quad (14)$$

Comparison with the linear optical schemes in Ref. [25].— Compared to the schemes using the zero-transmission law (ZTL) in Fourier transform interferometers in Ref. [25] (which we call ‘ZTL scheme’ from now on), our scheme is substantially more efficient for $N \geq 3$ both in the photon numbers and success probabilities. For $N = 2$ (qudit Bell state), our scheme has lower success probability ($d\left(\frac{d!}{d^d}\right)^4$ is smaller than $\frac{d(2d-1)!}{(2d+1)^{2d-1}}$ of the ZTL scheme) but requires less photons (we need $2d$ photons while the ZTL scheme needs $2d+1$).

Since the general ZTL scheme in Ref. [25] has a very low efficiency, an alternative near optimal scheme is proposed that can be applied to general N and d . We can see that the near-optimal

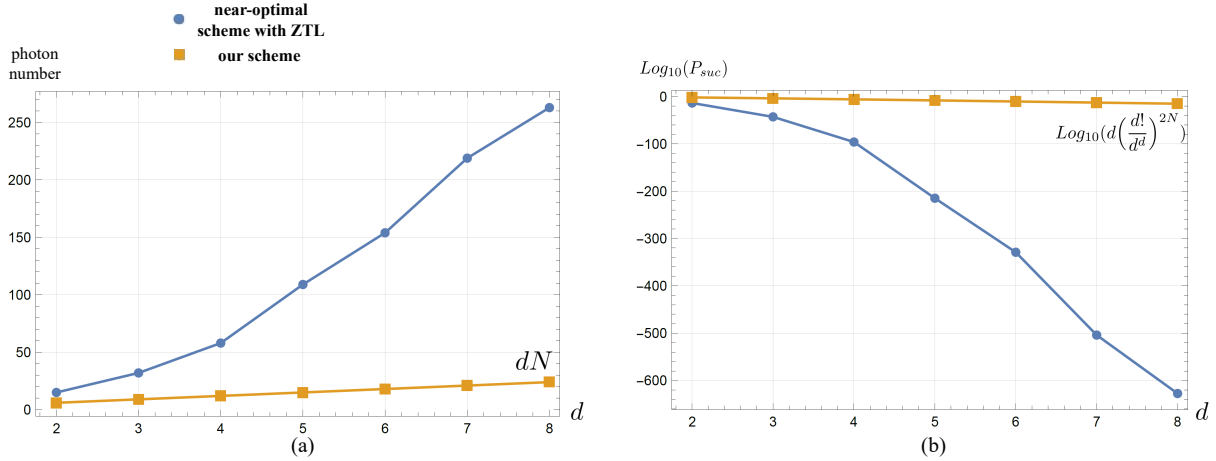


FIG. 4: Comparison of our scheme with the near-optimal scheme of Ref. [25] for $N = 3$ in (a) photon numbers, and (b) the logarithmic scales of the success probabilities. Graph (b) shows that the success probability is enhance exponentially in our scheme.

solution still needs significantly more photons and exponentially lower success probability than ours. Fig. 4 compares the required photon numbers and P_{suc} of the near-optimal ZTL scheme with ours for $N = 3$ and $2 \leq d \leq 8$. On the other hand, a brute-force method is also used in Ref. [25] for

$N = d = 3$ that diminishes the photon number to 25 with $P_{\text{suc}} \sim 10^{-10}$, which is still much less efficient than our scheme that requires 9 photons with $P_{\text{suc}} \sim 3.6 \times 10^{-4}$. The authors increased P_{suc} to $\sim 0.8 \times 10^{-4}$ with multiplexing, which however is still lower than a quarter of ours.

Construction of linear optical schemes in OAM and multi-rail encodings.— The linear optical logic gates in Fig. 1 can be implemented with any qudit encoding system of linear optics. Among them, we discuss the OAM and multi-rail encodings here.

In the OAM encoding, it is straightforward to establish the scheme, because the the OAM beam splitter [30] and OAM-only Fourier transformation operators [31] implement the CN_d and F_d gates respectively.

In the multi-rail encoding, a permutation of photon paths becomes the CN_d gate and the d -partite port that Fourier transforms the spatial states of photons becomes the F_d gate and Indeed, for $d = 3$ case, the multi-rail implementation of linear optical

elements are given by

$$\begin{array}{c}
 \text{CN}_3 = \begin{array}{c} \text{blue box} \\ \text{with ports} \end{array} \\
 \text{F}_3 = \begin{array}{c} \text{orange box} \\ \text{with ports} \end{array}
 \end{array}
 = \begin{array}{c} \text{circuit diagram} \\
 \text{with 3 inputs} \text{ 0, 1, 2 } \text{ and 3 outputs} \text{ 0, 1, 2 } \\
 \text{and internal lines labeled 0, 1, 2} \end{array}
 \quad , \quad (15)$$

which can be directly generalized to any d -level systems. Replacing all the linear optical logic gates in Fig. 3 with the operators in (15), we obtain a circuit for the $N = 3$ qutrit GHZ state in the multirail encoding as in Fig. 5.

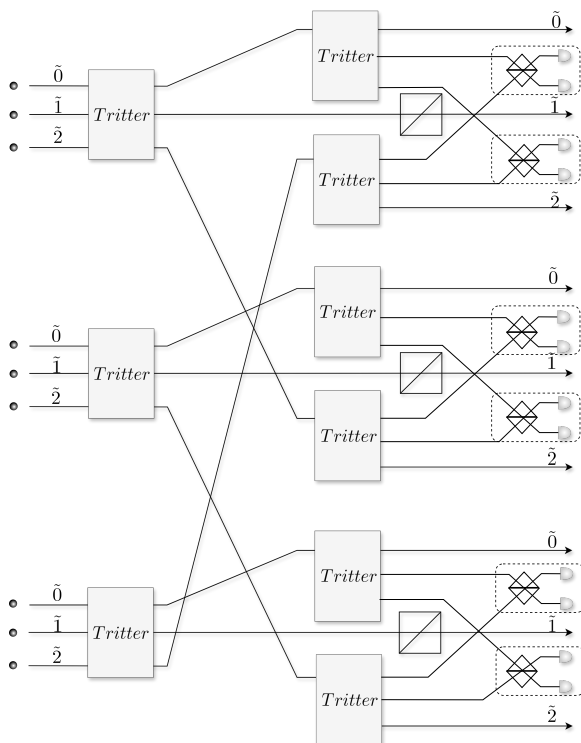


FIG. 5: $N = d = 3$ GHZ generation circuit in the multirail encoding example.

An advantage of the multirail encoding circuit is that CN_d and \overline{CN}_d is achieved with the permutation of paths, hence the final circuit consists of simpler optical elements, i.e., d -partite ports including BSs, permutations of paths, and photon detectors.

Discussions.— Our scheme has several manifest advantages in using the qudit GHZ state as a resource for high-dimensional quantum information processing. First, as we have already demonstrated, our scheme enables more efficient generations of the resource states with single-photons and linear operators, which becomes a more feasible resource state that can generate qudit cluster states with fusion gates for the qudit MBQC [23–25]. Second, our scheme is adequate to verify the optimal state for the violation of Bell-CHSH nonlocality test. While the maximally entangled state entails the maximal Bell-CHSH violation in $d = 2$ systems, the scenario becomes more complicated for higher dimensional systems. Ref. [12, 13] shows that the maximal Bell-CHSH violation occurs for a non-maximally entangled state, which is also verified numerically for the $N = d = 3$ case in Ref. [32]. Therefore, for the experiments of those maximal violations, schemes for

generalized qudit GHZ states with relatively asymmetric amplitudes are indispensable. Our scheme easily achieve the condition by varying the transitivity of beamsplitters. Third, our scheme consists of linear optical logic gates that any type of qubit encoding (e.g., optical angular momentum (OAM), multi-rail, time-bin, etc.) can realize.

In addition, the methodology of composing linear optical logic gates based on the LQG picture can be useful to find more general types of qudit multipartite entanglement. For example, Ref. [33] proposed heralded schemes for N -partite N -level symmetric and anti-symmetric states based on the method. We expect to construct more rigorous and general formalism of the LQG picture that will provide a more systematic path for the heralded generations of essential qudit entanglement such as absolutely maximally entangled (AME) states.

Acknowledgements.— SC is grateful to Prof. Jung-Hoon Chun for his support on this research. SC is supported by National Research Foundation of Korea (NRF, 2019R1I1A1A01059964, RS-2023-00245747). JR acknowledges support from the National Research Foundation (NRF) of Korea grant funded by the Korea Government (Grant No. NRF-2022M3K2A1083890). YSK acknowledges support from the KIST institutional program (2E32941).

* sbthesy@skku.edu

- [1] Costantino Budroni, Adán Cabello, Otfried Gühne, Matthias Kleinmann, and Jan-Ake Larsson. Kochen-specker contextuality. *Rev. Mod. Phys.*, 94:045007, Dec 2022.
- [2] Francesco Tacchino, Alessandro Chiesa, Roberta Sessoli, Ivano Tavernelli, and Stefano Carretta. A proposal for using molecular spin qudits as quantum simulators of light–matter interactions. *Journal of Materials Chemistry C*, 9(32):10266–10275, 2021.
- [3] Simone Chicco, Giuseppe Allodi, Alessandro Chiesa, Elena Garlatti, Christian D Buch, Paolo Santini, Roberto De Renzi, Stergios Piligkos, and Stefano Carretta. Proof-of-concept quantum simulator based on molecular spin qudits. *Journal of the American Chemical Society*, 146(1):1053–1061, 2023.
- [4] Peter W Shor. Algorithms for quantum computation: discrete logarithms and factoring. In *Proceedings 35th annual symposium on foundations of computer science*, pages 124–134. Ieee, 1994.
- [5] Charles H Bennett, Gilles Brassard, Claude Crépeau, Richard Jozsa, Asher Peres, and William K Wootters. Teleporting an unknown quantum state via dual classical and einstein-podolsky-rosen channels. *Physical Review Letters*,

70(13):1895, 1993.

[6] Nathan K Langford, Rohan B Dalton, Michael D Harvey, Jeremy L O'Brien, Geoffrey J Pryde, Alexei Gilchrist, Stephen D Bartlett, and Andrew G White. Measuring entangled qutrits and their use for quantum bit commitment. *Physical Review Letters*, 93(5):053601, 2004.

[7] Alipasha Vaziri, Gregor Weihs, and Anton Zeilinger. Experimental two-photon, three-dimensional entanglement for quantum communication. *Physical Review Letters*, 89(24):240401, 2002.

[8] Adetunmise C Dada, Jonathan Leach, Gerald S Buller, Miles J Padgett, and Erika Andersson. Experimental high-dimensional two-photon entanglement and violations of generalized bell inequalities. *Nature Physics*, 7(9):677–680, 2011.

[9] Bart-Jan Pors, Filippo Miatto, ER Eliel, JP Woerdman, et al. High-dimensional entanglement with orbital-angular-momentum states of light. *Journal of Optics*, 13(6):064008, 2011.

[10] Manuel Erhard, Mario Krenn, and Anton Zeilinger. Advances in high-dimensional quantum entanglement. *Nature Reviews Physics*, 2(7):365–381, 2020.

[11] Michael Walter, David Gross, and Jens Eisert. Multipartite entanglement. *Quantum Information: From Foundations to Quantum Technology Applications*, pages 293–330, 2016.

[12] Daniel Collins, Nicolas Gisin, Noah Linden, Serge Massar, and Sandu Popescu. Bell inequalities for arbitrarily high-dimensional systems. *Physical Review Letters*, 88(4):040404, 2002.

[13] Antonio Acin, Thomas Durt, Nicolas Gisin, and José Ignacio Latorre. Quantum nonlocality in two three-level systems. *Physical Review A*, 65(5):052325, 2002.

[14] Mercedes Gimeno-Segovia, Pete Shadbolt, Dan E Browne, and Terry Rudolph. From three-photon greenberger-horne-zeilinger states to ballistic universal quantum computation. *Physical Review Letters*, 115(2):020502, 2015.

[15] FV Gubarev, IV Dyakonov, M Yu Saygin, GI Struchalin, SS Straupe, and SP Kulik. Improved heralded schemes to generate entangled states from single photons. *Physical Review A*, 102(1):012604, 2020.

[16] Shuai Zhao, Wen-Fei Cao, Yi-Zheng Zhen, Changchen Chen, Li Li, Nai-Le Liu, Feihu Xu, and Kai Chen. Higher amounts of loophole-free bell violation using a heralded entangled source. *New Journal of Physics*, 21(10):103008, 2019.

[17] Morgan M Weston, Sergei Slussarenko, Helen M Chrzanowski, Sabine Wollmann, Lynden K Shalm, Varun B Verma, Michael S Allman, Sae Woo Nam, and Geoff J Pryde. Heralded quantum steering over a high-loss channel. *Science advances*, 4(1):e1701230, 2018.

[18] Nicolas J Cerf, Serge Massar, and Stefano Pironio. Greenberger-Horne-Zeilinger paradoxes for many qudits. *Physical Review Letters*, 89(8):080402, 2002.

[19] Jinhyoung Lee, Seung-Woo Lee, and Myungshik S Kim. Greenberger-Horne-Zeilinger nonlocality in arbitrary even dimensions. *Physical Review A*, 73(3):032316, 2006.

[20] Weidong Tang, Sixia Yu, and CH Oh. Greenberger-Horne-Zeilinger paradoxes from qudit graph states. *Physical Review Letters*, 110(10):100403, 2013.

[21] Junghee Ryu, Changhyoup Lee, Marek Źukowski, and Jinhyoung Lee. Greenberger-Horne-Zeilinger theorem for N qudits. *Physical Review A*, 88(4):042101, 2013.

[22] Wonmin Son, Jinhyoung Lee, and MS Kim. Generic bell inequalities for multipartite arbitrary dimensional systems. *Physical Review Letters*, 96(6):060406, 2006.

[23] Yi-Han Luo, Han-Sen Zhong, Manuel Erhard, Xi-Lin Wang, Li-Chao Peng, Mario Krenn, Xiao Jiang, Li Li, Nai-Le Liu, Chao-Yang Lu, et al. Quantum teleportation in high dimensions. *Physical Review Letters*, 123(7):070505, 2019.

[24] Chenyu Zhang, JF Chen, Chaohan Cui, Jonathan P Dowling, ZY Ou, and Tim Byrnes. Quantum teleportation of photonic qudits using linear optics. *Physical Review A*, 100(3):032330, 2019.

[25] Stefano Paesani, Jacob FF Bulmer, Alex E Jones, Raffaele Santagati, and Anthony Laing. Scheme for universal high-dimensional quantum computation with linear optics. *Physical Review Letters*, 126(23):230504, 2021.

[26] Wen-Bo Xing, Xiao-Min Hu, Yu Guo, Bi-Heng Liu, Chuan-Feng Li, and Guang-Can Guo. Preparation of multiphoton high-dimensional GHZ states. *Optics Express*, 31(15):24887–24896, 2023.

[27] Thomas J Bell, Jacob FF Bulmer, Alex E Jones, Stefano Paesani, Dara PS McCutcheon, and Anthony Laing. Protocol for generation of high-dimensional entanglement from an array of non-interacting photon emitters. *New Journal of Physics*, 24(1):013032, 2022.

[28] Seungbeom Chin, Yong-Su Kim, and Marcin Karczewski. Shortcut to multipartite entanglement generation: A graph approach to boson subtractions. *arXiv preprint arXiv:2211.04042*, 2022.

[29] Seungbeom Chin. From linear quantum system graphs to qubit graphs: Heralded generation of graph states. *arXiv preprint arXiv:2306.15148*, 2023.

[30] XuBo Zou and W Mathis. Scheme for optical implementation of orbital angular momentum beam splitter of a light beam and its application in quantum information processing. *Physical Review A*, 71(4):042324, 2005.

[31] Jaroslav Kysela, Xiaoqin Gao, and Borivoje Dakić. Fourier transform of the orbital angular momentum of a single photon. *Physical Review Applied*, 14(3):034036, 2020.

[32] Wiesław Laskowski, Junghee Ryu, and Marek Źukowski. Noise resistance of the violation of local causality for pure three-qutrit entangled states. *Journal of Physics A: Mathematical and Theoretical*, 47(42):424019, 2014.

- [33] Seungbeom Chin. Creating highly symmetric qudit heralded entanglement through highly symmetric graphs. *arXiv preprint arXiv:2404.05273*, 2024.
- [34] Seungbeom Chin, Yong-Su Kim, and Sangmin Lee. Graph picture of linear quantum networks and entanglement. *Quantum*, 5:611, 2021.
- [35] Seungbeom Chin, Marcin Karczewski, and Yong-Su Kim. From graphs to circuits: Optical heralded generation of N -partite GHZ and W states. *arXiv preprint arXiv:2310.10291*, 2023.

Appendix A: Operations of CN_d , the d -level CNOT gate between the spatial mode and the internal state

Unlike the conventional generalized CNOT gate that works on two different qudits, CN_d and \overline{CN}_d here transform the spatial mode of a given photon according to its internal state. They transform the two variables in the same way as the generalized CNOT gate between two qudits. The spatial mode and internal state play the role of the target and control states.

More explicitly, the operation of CN_d given by Eqs. (2) can be enumerated as the following table:

$ \tilde{0}\rangle_0 \rightarrow \tilde{0}\rangle_0$	$ \tilde{1}\rangle_0 \rightarrow \tilde{1}\rangle_1$	\dots	$ \tilde{d-1}\rangle_0 \rightarrow \tilde{d-1}\rangle_{d-1}$
$ \tilde{0}\rangle_1 \rightarrow \tilde{1}\rangle_1$	$ \tilde{1}\rangle_1 \rightarrow \tilde{1}\rangle_2$	\dots	$ \tilde{d-1}\rangle_1 \rightarrow \tilde{d-1}\rangle_0$
\vdots	\vdots	\vdots	\vdots
$ \tilde{0}\rangle_{d-2} \rightarrow \tilde{0}\rangle_{d-2}$	$ \tilde{1}\rangle_{d-2} \rightarrow \tilde{1}\rangle_{d-1}$	\dots	$ \tilde{d-1}\rangle_{d-2} \rightarrow \tilde{d-1}\rangle_{d-3}$
$ \tilde{0}\rangle_{d-1} \rightarrow \tilde{0}\rangle_{d-1}$	$ \tilde{1}\rangle_{d-1} \rightarrow \tilde{1}\rangle_0$	\dots	$ \tilde{d-1}\rangle_{d-1} \rightarrow \tilde{d-1}\rangle_{d-2}$

Comparing the transformations in the same row of the table, we can see that that CN_d splits photons of different internal states in the same spatial mode into different spatial modes.

Appendix B: Comprehensive analysis on the qudit N -partite GHZ state generation scheme

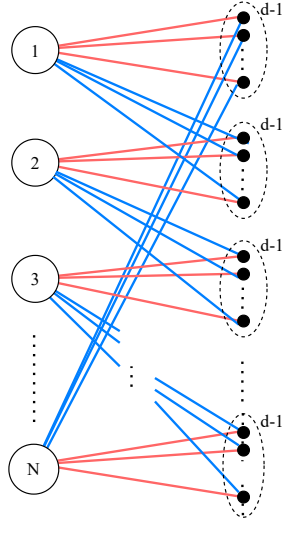
Here we provide a comprehensive explanation on the linear optical circuit for generating the qudit GHZ state given in Fig. 2. We first explain how we designed our scheme based on the graph picture of linear quantum networks (the LQG picture) [28, 34] and then show that the scheme indeed generates the expected target state.

1. Construction of linear optical circuit from the boson subtraction operator

Our scheme can be considered a linear optical realization of the boson subtraction scheme in Ref. [28], which exploited the LQG picture [28, 34] to find boson subtraction schemes for generating multipartite entanglement of qubits and qudits. Those boson subtraction schemes are in principle realized as linear optical heralded circuits, which is elucidated as a set of direct translation rule for qubit cases in Ref. [35]. However, its general extension to arbitrary d -level cases is absent.

In Ref. [28], the bipartite graph (bigraph) that corresponds to the boson subtraction scheme for the qudit

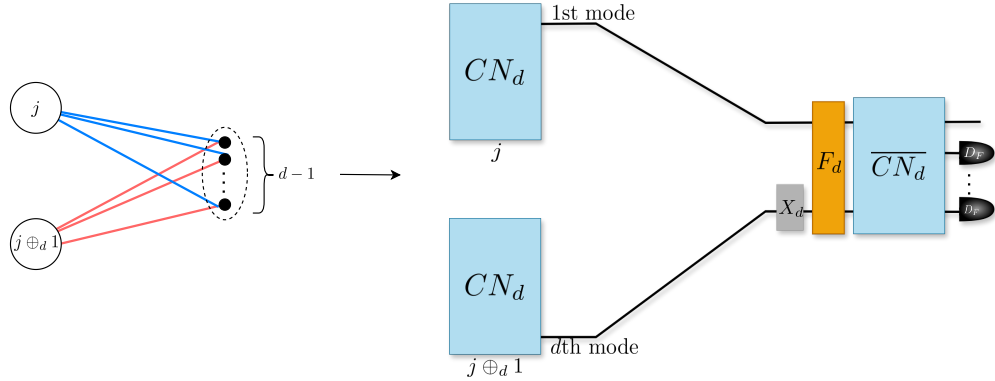
GHZ state is given by



which corresponds to the following operator (see Table I of Ref. [28]):

$$\hat{A}_{N,d} = \left(\frac{1}{\sqrt{2}}\right)^{(d-1)N} (\hat{a}_{1,0} - \hat{a}_{2,\widetilde{d-1}})^{d-1} (\hat{a}_{2,0} - \hat{a}_{3,\widetilde{d-1}})^{d-1} (\hat{a}_{3,0} - \hat{a}_{4,\widetilde{d-1}})^{d-1} \cdots \times (\hat{a}_{N,0} - \hat{a}_{1,\widetilde{d-1}})^{d-1}. \quad (B1)$$

We can intuitively see that the following translation holds from the LQG picture to the linear optical system:



Therefore, by combining the N sets of the above linear optical element with the structure of the bigraph (B1), we obtain the scheme in Fig. 2 that generates the expected target state.

2. Demonstrations of the final state generated by the scheme in Fig. 2

To demonstrate that the scheme in Fig. 2 generates the qudit GHZ state, we need the following two identities that were first given in Ref. [28] without proofs. Due to their significance in calculating our circuit operation, we restate them here with proofs.

Identity 1. For $l \in \{0, 1, \dots, d-1\}$,

$$(\hat{a}_0)^l (\hat{a}_{\widetilde{d-1}})^{d-1-l} \prod_{s=0}^{d-1} \hat{a}_s^\dagger |vac\rangle = (-1)^{d-1-l} \frac{l!(d-1-l)!}{\sqrt{d}^{d-2}} \hat{a}_{\widetilde{d-1-l}}^\dagger |vac\rangle \quad (B2)$$

Proof.

$$\begin{aligned}
& (\hat{a}_0)^l (\hat{a}_{\widetilde{d-1}})^{d-1-l} \prod_{s=0}^{d-1} \hat{a}_s^\dagger |vac\rangle \\
&= \frac{1}{\sqrt{d}^{d-1}} (\hat{a}_0 + \hat{a}_1 + \cdots + \hat{a}_{d-1})^l (\hat{a}_0 + \omega \hat{a}_1 + \cdots + \omega^{d-1-l} \hat{a}_{d-1})^{d-1-l} \prod_{s=0}^{d-1} \hat{a}_s^\dagger |vac\rangle \\
&= \frac{1}{\sqrt{d}^{d-1}} (\hat{a}_0 + \hat{a}_1 + \cdots + \hat{a}_{d-1})^l (d-1-l)! \sum_{\substack{j_1 \neq j_2 \neq \cdots \\ \neq j_{d-1-l} \\ =0}}^{d-1} \omega^{j_1+j_2+\cdots+j_{d-1-l}} \hat{a}_{j_1} \hat{a}_{j_2} \cdots \hat{a}_{j_{d-1-l}} \prod_{s=0}^{d-1} \hat{a}_s^\dagger |vac\rangle \\
&= \frac{l!}{\sqrt{d}^{d-1}} \sum_{\substack{j_1 \neq j_2 \neq \cdots \\ \neq j_{d-1-l} \\ =0}}^{d-1} \omega^{j_1+j_2+\cdots+j_{d-1-l}} \left(\sum_{q=0}^{d-1} \hat{a}_q^\dagger - \hat{a}_{j_1}^\dagger - \hat{a}_{j_2}^\dagger - \cdots - \hat{a}_{j_{d-1-l}}^\dagger \right) |vac\rangle
\end{aligned} \tag{B3}$$

Using

$$\sum_{\substack{j_1 \neq j_2 \neq \cdots \\ \neq j_{d-1-l} \\ =0}}^{d-1} \omega^{j_1+j_2+\cdots+j_{d-1-l}} = (-1)^{d-1-l} \sum_{j=0}^{d-1} \omega^{(d-1-l)} = 0, \tag{B4}$$

Eq. (B3) becomes

$$\begin{aligned}
& - \frac{l!}{\sqrt{d}^{d-1}} \sum_{\substack{j_1 \neq j_2 \neq \cdots \\ \neq j_{d-1-l} \\ =0}}^{d-1} \omega^{j_1+j_2+\cdots+j_{d-1-l}} (\hat{a}_{j_1}^\dagger + \hat{a}_{j_2}^\dagger + \cdots + \hat{a}_{j_{d-1-l}}^\dagger) |vac\rangle \\
&= - \frac{l!}{\sqrt{d}^{d-1}} (d-1-l) \sum_{\substack{j_1 \neq j_2 \neq \cdots \\ \neq j_{d-1-l} \\ =0}}^{d-1} \omega^{j_1+j_2+\cdots+j_{d-1-l}} \hat{a}_{j_1}^\dagger \\
&= (-1)^{d-1-l} \frac{l!(d-1-l)!}{\sqrt{d}^{d-1}} \sum_{j_1=0}^{d-1} \omega^{(d-1-l)j_1} \hat{a}_{j_1}^\dagger \\
&= (-1)^{d-1-l} \frac{l!(d-1-l)!}{\sqrt{d}^{d-2}} \hat{a}_{\widetilde{d-1-l}}^\dagger |vac\rangle.
\end{aligned} \tag{B5}$$

□

Identity 2. For $m \in \{1, \dots, d-1\}$,

$$(\hat{a}_0)^m (\hat{a}_{\widetilde{d-1}})^{d-m} \prod_{s=0}^{d-1} \hat{a}_s^\dagger |vac\rangle = 0 \tag{B6}$$

Proof. It is directly derived from Identity 1. □

There are N spatial subsystems that has d modes respectively in Fig. 2, hence the photon creation operator is denoted as $\hat{a}_{k,s}^{j\dagger}$, which denotes that a photon is in the j th subsystem, k th mode, and s th internal state. The d photons with orthogonal qudit states are injected into each spatial subsystem. Hence the initial state is given by

$$\prod_{j=1}^N (\hat{a}_{0,0}^{j\dagger} \hat{a}_{0,1}^{j\dagger} \cdots \hat{a}_{0,d-1}^{j\dagger}) |vac\rangle. \tag{B7}$$

Identities 1 and 2 show that when the photons pass through CN_d gates, the only case when one photon goes to X_{d-1-l}^j ($l \in \{1, 2, \dots, d-2\}$) is when l photons goes to $\hat{a}_{0,\tilde{0}}^{1\dagger}$ and $(d-1-l)$ photons goes to $\hat{a}_{d-1,\tilde{d}-1}^{1\dagger}$. This property can be used to verify all the surviving terms after the postselection by D_{FS} .

First, suppose that the d photons in subsystem 1 goes to mode 0 ($(\hat{a}_{0,\tilde{0}}^{1\dagger})^d$). Then by the postselections at D_{FS} , the only case that survives is that each set of d photons in all subsystems goes to mode 0, which corresponds to the term $|\underbrace{0, 0, \dots, 0}_N\rangle$. Second, suppose that the d photons in subsystem 1 goes to mode (d-1) ($(\hat{a}_{0,\tilde{d}-1}^{1\dagger})^d$). By the same reasoning, the only surviving term under the postselection is $|\underbrace{d-1, d-1, \dots, d-1}_N\rangle$. Third, suppose that among d photons in subsystem 1, the l photons goes to $\hat{a}_{0,\tilde{0}}^{1\dagger}$, $(d-1-l)$ photons to $\hat{a}_{d-1,\tilde{d}-1}^{1\dagger}$, hence one photon to X_{d-1-l}^1 ($(\hat{a}_{0,\tilde{0}}^{1\dagger})^l (\hat{a}_{0,\tilde{d}-1}^{1\dagger})^{d-1-l} \hat{a}_{0,\tilde{d}-1-l}^{1\dagger}$). We can check that the surviving term to satisfy the postselection condition is $|\underbrace{d-1-l, d-1-l, \dots, d-1-l}_N\rangle$. Fourth, if more than two photons go to X_{d-1-l}^1 , there is no term that fulfill the postselection condition. All in all, the final state after the postselections of D_{FS} is given by

$$\frac{1}{d^{Nd}} \left((d!)^N |0, 0, \dots\rangle + (d!)^N |d-1, d-1, \dots, d-1\rangle + (d! \sqrt{d} \alpha)^N \sum_{k=1}^{d-2} |k, k, \dots, k\rangle \right) \quad (B8)$$

By setting $\alpha = \frac{1}{\sqrt{d}}$, i.e., placing $1 : (d-1)$ BSs on X_l^j ($j \in \{1, \dots, N\}$, $l \in \{1, \dots, d-2\}$), the final state becomes $|GHZ\rangle_N^d$ as expected. The success probability is given by

$$P_{suc}(N, d) = d \left(\frac{d!}{d^d} \right)^{2N}. \quad (B9)$$